The Analysis of Interference Effects in the Sum Frequency Spectra of Water Interfaces†

Mac G. Brown, Elizabeth A. Raymond, Heather C. Allen, Lawrence F. Scatena, and Geraldine L. Richmond*

Department of Chemistry, University of Oregon, Eugene, Oregon 97403

Received: March 23, 2000; In Final Form: May 19, 2000

Vibrational sum frequency (VSF) spectroscopy has been increasingly used in recent years to measure the vibrational spectroscopy of molecules at surfaces. Some of the more important systems examined in such studies involve the surface of liquid water. Unfortunately, obtaining spectral fits to vibrational spectra acquired in these studies can be challenging. The difficulty arises from the wide range of contributing vibrational modes, the breadth of the spectral peaks for hydrogen-bonded water molecules, and the complex interference effects that can arise between adjacent vibrational modes because of the coherent nature of the sum frequency process. In this paper, we describe a detailed method for obtaining spectral fits to such VSF data that takes into account a range of water species present at a water surface and the possible interference between these contributing modes. The relationship between the spectral information derived and the molecular orientation is also given. This analysis is applied to two cases, VSF spectra of water measured at the CCl_4/H_2O interface and at the air/H_2O interface.

Introduction

The structure of water at interfaces is an important, yet notoriously difficult, field of study. It is only with techniques developed in the past few years, such as vibrational sum frequency spectroscopy (VSFS), that high-quality spectra of molecular species at water interfaces have been obtained.[1−12] The interfacial vibrational spectrum of water is of particular interest, as the hydrogen-bond interaction is highly sensitive to the local molecular environment.[13] The water vibrational spectrum, therefore, provides a sensitive probe of the structure and energetics of the hydrogen-bond network at the interface. The sensitivity of VSFS to water vibrational modes is accompanied by a complexity in spectral interpretation. This is because of the variety of different environments of the interfacial water molecules and the broad nature of the peaks corresponding to water molecules that are extensively hydrogen-bonded to other water molecules. This difficulty in interpretation is not unique to the vibrational spectroscopy at surfaces but has been a major point of controversy over past decades in the interpretation of bulk water spectra.[13−15]

Because of the coherent nature of sum frequency generation, the vibrational spectra obtained can exhibit complex interference patterns from the broad overlapping peaks that complicate the analysis.[5−7] Interestingly, however, the coherent nature of the sum frequency response means that a complete analysis of VSF spectra provides information on the average orientation of the molecules at the interface in addition to the energy of vibrational modes.[16,17]

In this paper, we provide details of the most comprehensive fit and analysis to date of the O−H stretch region of surface water obtained in VSFS studies. The analysis integrates spectroscopic characteristics of the O−H stretch region obtained in IR and Raman studies of bulk water with VSF concepts developed and applied[7,16,17] to the analysis of CH_2/CH_3 vibrational modes. We have applied this integrated analysis to the VSF spectra of surface H_2O from two systems, the CCl_4/water and air/water interfaces. The motivation for developing an analysis of this type has been two-fold. In the past year, work in this laboratory has generated VSF spectra of surface water that show evidence for interfacial water species heretofore not observed.[9,10] Second, such an analysis contributes to the understanding of previously unresolved spectral features in air/water studies that will aid in the analysis of future surface water studies of these and other systems.

The paper begins with a description of the analysis procedure used in this study and, most importantly, the steps necessary to apply this procedure to the VSF spectra of water interfaces. This is followed by application of the procedure to the VSF spectra of two systems. The first is the CCl_4/water interface, a system that displays the widest range of water environments yet studied. The VSF spectrum of water at this interface[10] is shown in Figure 1a. Recent experiments[10] show that this interface is dominated by water species that show either no hydrogen bonding with other water molecules or hydrogen bonding through only one of the two OH groups in the molecule, thereby yielding dangling bonds. Water molecules are present at the interface with higher coordination, but they are observed in smaller numbers than the former. The second spectrum analyzed is that corresponding to the air/water interface[9] and is shown in Figure 1b. This interface has been examined by VSF in previous studies,[1,2,18,19] but it is only in the recent studies from this laboratory that features corresponding to oriented, weakly associated, "vapor-phase" molecules at the interface have been resolved. The analysis is applied to these spectral features as well as to the modes of highly coordinated water molecules and the dangling bond mode. The analysis provides the spectral deconvolution necessary to understand this and future spectra and also shows how the orientation of interfacial molecules can be derived.

† Part of the special issue "C. Bradley Moore Festschrift".
* Author to whom correspondence should be addressed.

10.1021/jp0010942 CCC: $19.00
Published on Web 07/21/2000

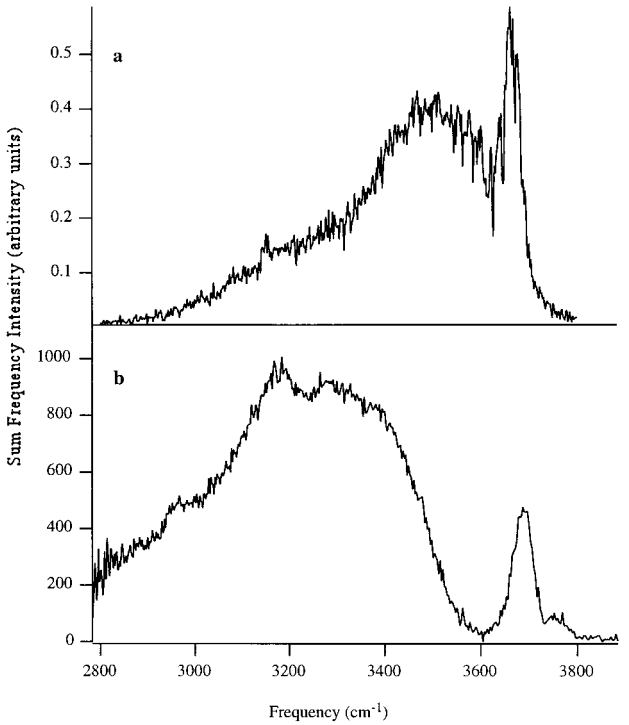

Figure 1. (a) VSF spectrum of the CCl_4/water interface. The sum frequency intensity at ~3650 cm^{-1} for this interface provides evidence for a considerable number of loosely hydrogen-bonded water molecules. (b) VSF spectrum of the air/water interface using the picosecond laser system described in the text. The small peak to the blue of the "free O−H" vibrational transition at 3702 cm^{-1} is assigned to the asymmetric stretch of "vapor-phase" water molecules, water oriented by, but only loosely associated with, the surface. Each of the spectra shown were recorded using SSP polarization conditions; correcting the spectra for dispersion through the use of Fresnel coefficients was not found to change the general spectral features observed.

Sum Frequency Generation

Sum frequency generation (SFG) is a second-order nonlinear optical process forbidden in media with inversion symmetry.[6] The inversion symmetry of a substance is naturally broken at an interface; therefore, SFG can be used as a surface-specific probe. These principles underlie the technique of VSFS, in which the vibrational spectroscopy of interfacial species is obtained by mixing light from a tunable IR source that scans over the vibrational modes of interest with light from a fixed-frequency visible laser at an interface. The resulting SF spectrum corresponds to the vibrational spectrum of the interfacial molecules. The intensity of the SFG light is related to the second-order susceptibility of the medium at the interface, $\chi^{(2)}$, and the intensity of the two input fields $I(\omega_{IR})$ and $I(\omega_{vis})$

$$I(\omega_{SFG}) \propto |\chi^{(2)}|^2 I(\omega_{IR}) I(\omega_{vis}) \quad (1)$$

where $\omega_{SFG} = \omega_{IR} + \omega_{vis.}$ Generally, the intensity of the sum frequency light generated by this process under nonresonant conditions is very weak and difficult to detect for molecular surfaces such as water. However, when the frequency of the tunable infrared light, ω_{IR}, approaches a vibrational resonance of the molecules at the interface, the generation of sum frequency light increases significantly. The second-order susceptibility of a medium can be conveniently broken down into a sum of nonresonant and vibrationally resonant terms for each vibrational mode υ

$$\chi^{(2)} = \chi^{(2)}_{NR} + \sum_{\upsilon} \chi^{(2)}_{\upsilon} \quad (2)$$

where the subscript NR refers to the nonresonant component of $\chi^{(2)}$ and ω_{vis} is assumed to be far from resonant with any electronic transitions.

It should be noted that the intensity of the SF light generated depends on the absolute square of $\chi^{(2)}$; thus, interference between different vibrations of similar energies is expected and can play a major role in the overall shape of the observed spectra. Interestingly, quantum mechanics even allows the sum frequency signal generated by the vibrations of different molecular species to interfere with one another. If a Lorentzian distribution of vibrational energies is assumed, each vibrational transition can be represented by the expression

$$\chi^{(2)}_{\upsilon} = \frac{A_{\upsilon}}{\omega_{IR} - \omega_{\upsilon} - i\Gamma_{\upsilon}} \quad (3)$$

where A_υ, ω_υ and Γ_υ are fit parameters corresponding to the amplitude, frequency, and damping constant, respectively, of the υth vibrational mode of the interface. Lorentzian line shapes are commonly used to take into account the interference between different vibrations, although other, more complex line shapes are also used. The broad "wings" characteristic of a Lorentzian distribution often overestimate the amount of overlap, and therefore the interference, between widely separated peaks. Particularly useful, although computationally more intensitive, is the lineshape profile described by Goates et al.[21] Similar to a Voigt profile, this lineshape expression is a convolution of eq 3 and a Gaussian distribution that attempts to take into account inhomogeneous broadening.[20,21] In this paper, this more complicated profile is used to describe vibrational features of the spectra, with details given in the section corresponding to the individual fits.

The interference between different vibrations resulting from the coherent nature of the experiment make the analysis of SFG spectra somewhat more complicated than that of spectra recorded with linear spectroscopic techniques. However, this complexity can be exploited if a complete analysis of the VSF spectrum is employed that takes into account the phase of the sum frequency response from contributing vibrational modes.[7,8] In particular, it is possible to constrain the average orientation of the molecules at the surface by relating the macroscopic second-order susceptibility, $\chi^{(2)}$, of the system to the molecular hyperpolarizabilities, β, of the individual molecules at the interface.[16,17]

The vibrationally resonant hyperpolarizability of a molecule, β_υ, a molecular property, is often described through an expression similar to eq 3

$$\beta_{lmn,\upsilon} = \frac{\langle g|\alpha_{lm}|\upsilon\rangle\langle\upsilon|\mu_n|g\rangle}{\omega_{IR} - \omega_{\upsilon} + i\Gamma_{\upsilon}} \quad (4)$$

where l, m, and n represent the molecular inertial axes (a, b, and c); μ_n and α_{lm} represent the dipole and Raman vibrational transition moments, respectively; and a Lorentzian distribution of resonant transition energies is assumed.[6] The absolute square of β can be considered a sum frequency "transition probability". An energy diagram illustrating the interference between different vibrational modes in a typical sum frequency experiment is shown in Figure 2. It is interesting to compare the interference of different vibrations in a sum frequency experiment to those in the classic double-slit experiment. In both cases, particles

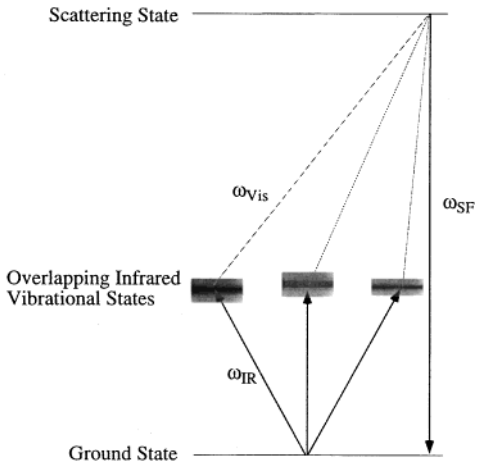

Figure 2. Energy diagram representative of a typical sum frequency transition exhibiting interference between different vibrations. In simplistic terms, the sum frequency response can be viewed as a combination of a resonant infrared transition with a nonresonant Raman transition. The overall process leaves the molecule in its original ground state. Interference patterns arise when different infrared transitions overlap, giving rise to multiple indistinguishable "paths" that give rise to the same sum frequency response.

traveling through *indistinguishable* intermediate states give rise to distinct interference patterns.[22]

The macroscopic property observed in sum frequency experiments, $\chi^{(2)}$, is a sum of the molecular hyperpolarizabililty over all of the molecules at the interface, taking into account the orientation of the different molecular species. Orientational information is obtained from the experimental spectra by considering how the observed Cartesian components of the macroscopic second-order susceptibility $\chi^{(2)}_{IJK,\upsilon}$ are derived from the corresponding spectroscopically active components of the molecular hyperpolarizability β_{lmn}. This is accomplished through an Euler angle rotation of the molecular axis system into the laboratory axis system, as defined through the use of the rotational matrix $\mu_{IJK:lmn}$. The general expression for the transformation from a molecular-fixed axis system to a laboratory-fixed axis system,[16,17] as given by Hirose et al., is

$$\chi^{(2)}_{IJK,\upsilon} = \sum_{lmn} \mu_{IJK:lmn} \cdot \beta_{lmn,\upsilon} \qquad (5)$$

The indices *I*, *J*, and *K* are replaced by the lab frame coordinates *X*, *Y*, or *Z* observed in a specific experiment. The indices *l*, *m*, and *n* run through the molecular coordinates *a*, *b*, and *c*. The orientation of the molecular axis system in the lab frame is defined by the transformation tensor, $\mu_{IJK:lmn}$ through the Euler angles θ, ϕ, and χ. The Euler angles are defined in Figure 3. If the signs of $\beta_{lmn,\upsilon}$ and $\chi^{(2)}_{IJK,\upsilon}$ are known, then the average orientation of the molecules can be constrained by analyzing how the sign of the transformation tensor changes with respect to the angles θ, ϕ, and χ. A comprehensive table of the appropriate transformation equations is given by Hirose et al. in their excellent general treatment of CH_2 and CH_3 vibrations in sum frequency spectra.[16,17] It should be noted that, here, the *b* axis is defined as the symmetry axis of the water molecule, and the hydrogens lie in the a−b plane, analogous to the treatment of C_{2v}-symmetric CH_2 groups by Hirose[17] in which the symmetry axis is considered to define the *c* axis. In the case of air/water and CCl_4/H_2O interfaces discussed here, the signs of the $\chi^{(2)}_{IJK,\upsilon}$ terms are known through a comprehensive fit of the observed sum frequency spectra to eqs 2 and 3, as described below, and the signs of the $\beta_{lmn,\upsilon}$ components are known through ab initio calculations.[5,23]

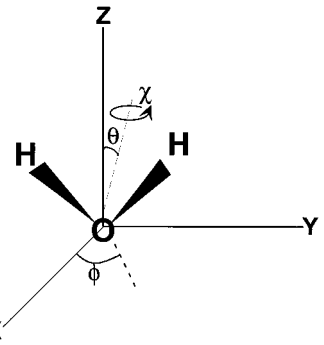

Figure 3. Definition of the Euler angles χ, θ, and ϕ. The angle θ, of most interest here, is defined as the angle between the symmetry axis of the water molecule and the *Z* axis of the laboratory frame. The *Z* axis in the laboratory frame is normal to the interface of interest with 0° pointing directly out of and 180° pointing directly into the water phase. ϕ and χ are rotations about the *Z* axis and about the symmetry axis of the molecule, respectively.

Experimental Section

The sum frequency spectra discussed here were obtained using the nanosecond and picosecond VSF laser systems at the University of Oregon. Each of the systems has been described elsewhere,[24−26] and so, only a brief description of the two systems is provided here. The spectra shown in Figure 1a,b were taken with S, S, and P polarization conditions for the sum frequency, visible, and infrared light, respectively.

The spectrum of the CCl_4/H_2O interface shown in Figure 1a was taken using a nanosecond SFG system recently developed by Scatena et al.[10] Briefly, the output of a Coherent Infinity Nd:YAG laser is used to drive the system. A portion of the 1064-nm output is frequency doubled for use as ω_{vis} and sent to the interface at the critical angle for total internal reflection. The remainder of the Nd:YAG output is directed into an OPO/OPA system where tunable infrared light from 1900 to 4000 cm^{-1} is generated and sent to the interface as ω_{IR}. The sum frequency light generated at each IR frequency is detected using a photomultiplier tube and boxcar integration.

The weak sum frequency signal observed at the air/water interface (Figure 1b) required the use of the higher laser peak powers generated by the picosecond VSF laser system developed by Gragson et al.[25,26] A cartoon of the air/water interfacial region is shown in Figure 4. The output of a Ti:sapphire laser at 800 nm is amplified and split, with approximately 25% of the output directed to the interface as ω_{vis}. The remaining 75% of the 800-nm light is used in an OPG and two-stage OPA system where tunable infrared light from 2700 to 4000 cm^{-1} is produced. The experiment was conducted using the external reflection geometry shown in Figure 4, and the sum frequency light generated is collected using a cooled CCD array.

Application of Analysis Principles

The vibrational spectrum of liquid water is notoriously difficult to interpret, with overlapping vibrational resonances spread over a large frequency range. The complexity displayed by such spectra is due to the many different local environments experienced by individual water molecules in the liquid. The spectra of water molecules at interfaces are no exception. A quick examination of the vibrational sum frequency spectra shown in Figure 1 for the CCl_4/water and air/water interfaces

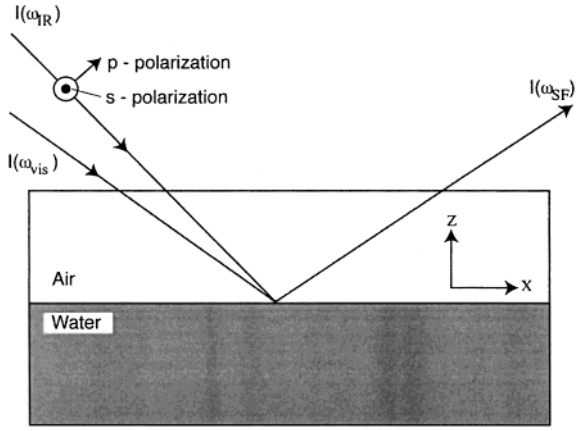

Figure 4. Diagram of a typical VSF experiment for air/water studies. A tunable infrared laser and a fixed-frequency visible laser are overlapped at an interface. Conservation of momentum gives rise to a well-defined sum frequency response to the combined input fields. Different polarization conditions can be chosen for the input and sum frequency lasers to probe different components of the second-order nonlinear susceptibility of the medium. In the spectra discussed in this work, S, S, and P polarization conditions were chosen for the sum frequency, visible, and infrared lasers, respectively.

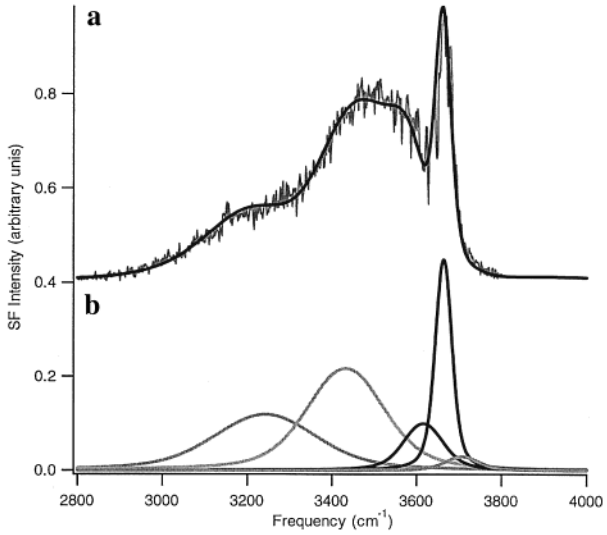

Figure 5. (a) Vibrational sum frequency spectrum of the CCl_4/water interface is shown with the accompanying nonlinear least-squares fit to the data. Each of the contributing vibrations is shown in Figure 5b. Vibrations fit with a negative amplitude are shown in gray, while vibrations with a positive amplitude are shown in black.

reveals a complex set of overlapping water O−H stretching vibrations spread over ∼700 cm^{-1}.

The vibrational frequency of an O−H intramolecular stretch is commonly associated with the strength of hydrogen bonding.[13] Intensity at lower vibrational energies (2900−3400 cm^{-1}) is assigned to the O−H symmetric stretch (SS) vibrations of tetrahedrally hydrogen-bonded water molecules. In infrared studies of bulk water, there are disagreements as to the specific water species contributing to the vibrational modes in this region, but generally the modes in this region have been simplistically described as "icelike" and "liquidlike" modes. The former, found at the lowest energies, corresponds to the cooperative vibrations of those water molecules that are symmetrically bonded to neighboring water molecules, whereas the latter corresponds to water molecules with asymmetric hydrogen bonding to other water molecules (SS−S modes and SS−AS modes respectively). For simplicity, we will use similar assignments in this region. Vibrational features in the high-energy region of the spectrum (3500−3800 cm^{-1}) are assigned to nontetrahedrally hydrogen-bonded molecules, water molecules that are only loosely associated with other water molecules, forming a vapor above the surface of liquid water. Interestingly, such weakly hydrogen-bonded vapor-phase molecules have been found at both the CCl_4/water and the air/water interfaces.

Intermediate between these two extremes are water molecules that straddle the interface with one O−H bond in the aqueous phase and the other protruding into the adjacent medium, participating in hydrogen bonding through only one O−H bond. The asymmetric bonding experienced by such water molecules creates two distinct vibrational modes, a sharp O−H vibration (called a "dangling bond" or a "free O−H" vibrational mode) at 3664 cm^{-1} (CCl_4/water)[10] and 3702 cm^{-1} (air/water)[9] and a somewhat broader vibrational mode at ∼3430 cm^{-1} corresponding to the bonded O−H mode of these interfacial water molecules (CCl_4/water).[10] Identification of these weakly hydrogen-bonded modes has been possible through a careful and lengthy comparison of the spectra shown here with Raman, infrared, and sum frequency studies of water and isotopic diluted solutions. Such analyses of the air/water[9] and CCl_4/water[10] sum frequency spectra have been reported elsewhere, and so, although crucial to any successful spectral fit, the details of the collected background information leading to individual peak assignments are only briefly presented here.

The analysis of a complex spectrum with a considerable number of overlapping vibrational modes, complicated further by a coherent spectroscopic technique sensitive to interference patterns between vibrations, can be quite intimidating. This process is discussed in some detail below for the CCl_4/water and air/water interfaces.

Application to the CCl_4/Water Interface. The vibrational sum frequency spectrum of the CCl_4/water interface is shown in Figure 5, with the nonlinear least-squares fit and the vibrations making up the spectrum shown. The CCl_4/water interface is both an interesting and a difficult spectrum to interpret, making it an excellent example for the procedure required to fit VSF spectra. The interaction of water and carbon tetrachloride can be considered a model that examines the details of water structure and dynamics when in contact with a slightly miscible hydrophobic phase, a model system applicable to a wide range of chemical and biological systems. It has long been suggested that the hydrogen-bond network of water becomes more structured, more icelike, at such a hydrophobic interface.[27,28] The water and carbon tetrachloride molecules are both fairly polarizable, with induced dipole moments at the interface considerably different from their bulk values, greatly complicating the theoretical models required for treatment of this system.[29]

The first, and perhaps most lengthy, step in the analysis of a sum frequency spectrum is to examine the literature for all applicable Raman- and infrared-active modes that might be contributing to the VSF spectral region. Table 1 contains five assigned modes derived in previous CCl_4/water spectral analysis.[10] The assignments include the symmetric and asymmetric stretches of water monomers found at the interface in these studies and the dangling bond and donor stretch modes of the water molecules that straddle the interface. A complex spectrum, such as that of the CCl_4/water interface, is described by a highly parametrized expression (eqs 2 and 3). Consequently, it can be difficult to decide whether a set of parameters determined by a fit are physically meaningful without additional information. For the CCl_4/water interface, this difficulty has largely been overcome through a complex series of experiments, as described by Scatena et al.[10] The next step in the process requires a careful

TABLE 1: Fit Parameters and Orientations Determined for the CCl_4/Water System[a]

	frequency (ω_v)[b]	width (Γ_v)[b]	amplitude (A_v)	orientation
SS−S (icelike)	3243	142	−0.35	$\theta > 90°$
donor with contributions from SS−A (liquidlike)	3433	107	−0.48	$\theta > 90°$
SS−water/CCl_4	3616	54	0.33	$\theta < 90°$
free OH	3664	23	0.75	$\theta < 90°$
AS−water/CCl_4	3708	43	−0.18	$\theta < 90°$

[a] Results from a nonlinear least-squares fit to the VSF spectrum of the CCl_4/water interface are shown. The spectrum was fit as described in the text. The phase (amplitude) of the free OH vibration is assigned a positive value. Orientational information is given in terms of the Euler angle θ, measured with respect to the water surface normal. It should be noted that some flexibility in adjusting individual parameters can give rise to equally good fits, however, the signs of the amplitudes, and hence the orientation information, were consistent through rigorous testing of other possibilities. [b] Frequencies and widths are in units of cm^{-1}.

nonlinear least-squares fit of the spectrum to eq 2, constraining known parameters. The spectrum of the CCl_4/water interface shown in Figure 5 was fit using a Levenberg−Marquardt nonlinear least-squares fitting scheme. Each vibrational resonance, $\chi_v^{(2)}$ is described by a convolution of a Gaussian distribution of frequencies and a homogeneous linewidth described by eq 3. The Gaussian line width is defined by considering the statistics of inhomogeneous broadening, whereas the Lorentzian line width arises from quantum mechanical homogeneous, or lifetime broadening. The spectra were fit assuming a constant homogeneous line width Γ of 2 cm^{-1}. This choice of line width is an arbitrary but reasonable choice, given normal vibrational lifetimes. The Gaussian or inhomogeneous line width was allowed to vary for each vibration. An excellent fit to the data was obtained by including only five vibrational transitions in the fit, representing contributions from water molecules on both sides of the interface and at the interfacial layer. To avoid complicating the analysis, as few modes as possible were used to describe the overlapping, tetrahedrally bonded vibrations seen in bulk studies. The vibrational modes determined from the previous work are shown in Figure 5, and information obtained from the fit is summarized in Table 1. The inclusion of a complex nonresonant hyperpolarizability term in the fit was attempted but was not found to improve the results significantly. Several of the peak parameters were constrained to certain value ranges through comparisons with infrared, Raman, and other sum frequency spectra, as described above.[10]

To obtain specific information on the orientation of the individual vibrational modes, it is necessary to determine the relative signs (phases) of the three parts of eq 4 for each vibration: the resonant second-order susceptibility, $\chi_v^{(2)}$, the spectroscopically active components of the molecular hyperpolarizability, β_v, and the transformation tensor μ. The sign of $\chi_v^{(2)}$ for each vibrational mode is determined from the nonlinear fit of the experimental spectrum. A simple group theoretical treatment of the water vibrational modes at the interface gives the following nonzero components of β_v:

$$\begin{aligned} C_{2v}\text{ symmetry symmetric stretches: } & \beta_{aab,v}, \beta_{bbb,v}, \beta_{ccb,v} \\ C_{2v}\text{ symmetry asymmetric stretches: } & \beta_{aba,v}, \beta_{baa,v} \\ C_{\infty v}\text{ symmetry stretches: } & \beta_{aab,v}, \beta_{bbb,v}, \beta_{ccb,v} \end{aligned} \quad (6)$$

The free O−H stretch at 3664 cm^{-1} and the accompanying bonded O−H stretch at ~3430 cm^{-1} are approximated as uncoupled vibrations of $C_{\infty v}$ symmetry for the purposes of this analysis, although assuming a lower degree of symmetry would not change the results. For the SSP polarization spectrum shown in Figure 5, the spectroscopically probed Cartesian components of $\chi^{(2)}$ are $\chi_{yyz}^{(2)}$ and $\chi_{yyx}^{(2)}$, as can be seen from an examination of Figure 5. If an isotropic distribution of the azimuthal angle is assumed, $\chi_{yyx}^{(2)}$ is zero by symmetry, leaving $\chi_{yyx}^{(2)}$ as the only observed component of $\chi^{(2)}$. In that case, eq 4 reduces to

$$\chi_{\mathrm{SSP},v}^{(2)} = \chi_{yyz,v}^{(2)} = \mu_{yyz:aab}\cdot\beta_{aab,v} + \mu_{yyz:bbb}\cdot\beta_{bbb,v} + \mu_{yyz:ccb}\cdot\beta_{ccb,v} \quad (7)$$

for the symmetric stretch of water, the free O−H stretch, and the bonded O−H stretch, for example. The expression for the asymmetric stretch of water is the following:

$$\chi_{\mathrm{SSP,as}}^{(2)} = \chi_{yyz,\mathrm{as}}^{(2)} = \mu_{yyz:aba}\cdot\beta_{aba,\mathrm{as}} + \mu_{yyz:baa}\cdot\beta_{baa,\mathrm{as}} \quad (8)$$

The sign of each component of β_v can be determined through ab initio calculation of the dipole moment derivatives $\partial\mu/\partial q_v$ and the zero-frequency polarizability derivatives $\partial\alpha/\partial q_v$.[5] These derivatives are positive in sign for the symmetric and asymmetric stretches of water, giving the same sign for each β_v component observed.[23] The sign of each transformation tensor element, μ, changes with respect to the Euler angles. A close examination of the tensor elements collected by Hirose et al.[16] reveals that the three elements $\mu_{yyz:aab}(\chi,\theta,\phi)$, $\mu_{yyz:ccb}(\chi,\theta,\phi)$, and $\mu_{yyz:bbb}(\chi,\theta,\phi)$ are in phase with each other when an isotropic average over the azimuthal angle, ϕ, is assumed. Each element μ is positive when the average value of θ for the excited molecules is from 0 to 90°, corresponding to the water hydrogens pointing toward the CCl_4 phase, and negative when the average value of θ is from 90 to 180°, corresponding to the hydrogens pointing back toward the water phase. The relative phases of $\chi^{(2)}$ and β are not found to depend on χ. The sign of the observed amplitude, A_v, of the corresponding $\chi_{yyz,v}^{(2)}$ term can therefore be directly related to the orientation of the vibrating molecule, experimentally constraining the possible average orientation of each vibration. An analysis of the asymmetric stretch gives the opposite result. Each element μ is negative when the average value of θ for the excited molecules is from 0 to 90° and positive when the average value of θ is from 90 to 180°. Water molecules oriented so as to give rise to a positive symmetric stretch should also have a corresponding negative asymmetric stretch, and vice versa. If we assign a positive phase to the free OH vibration, indicating that the dangling bond points away from the bulk water phase, the remaining vibrations can all be assigned specific relative phases. This analysis would suggest the orientations given in Table 1, assignments that are in agreement with molecular dynamics calculations.[29] It is important to note that the analysis of other observable polarization conditions of the second-order susceptibility, such as SPS spectra, gives different interference patterns, although the analysis of such spectra should give rise to the same orientation information. The interpretation of these spectra is difficult because of weak signal levels, but an attempt at an analysis is currently underway.

The Air/Water Interface. The procedure used to fit and analyze the sum frequency spectrum of the air/water interface is entirely analogous to that described above for the CCl_4/water interface. The sum frequency spectrum was recorded, and a nonlinear least-squares fit to a collection of interfering vibrational modes was obtained. An attempt was made to fit each vibration using a Lorentzian distribution, but the results were found to be generally unsatisfactory. The broad tails of the

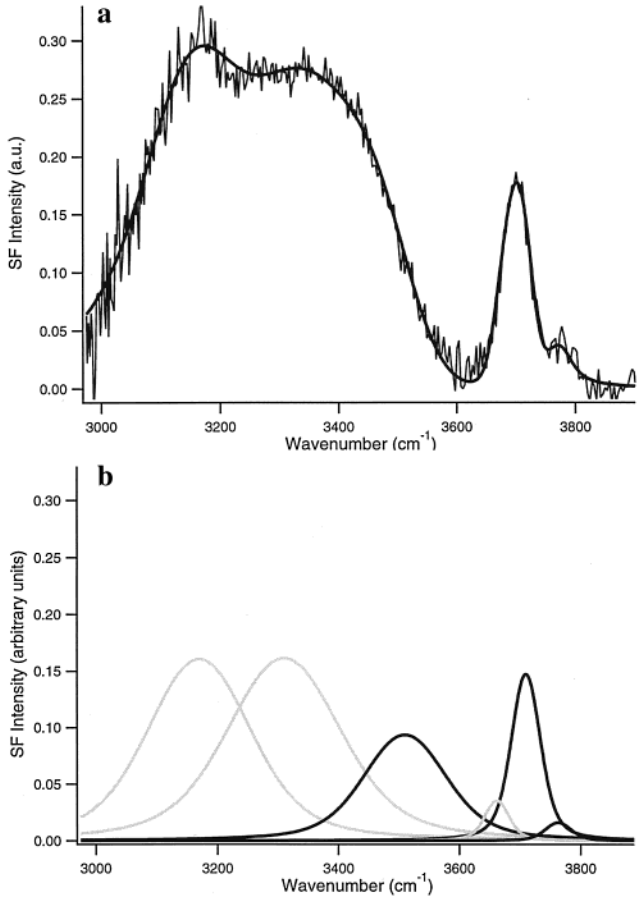

Figure 6. (a) Vibrational sum frequency spectrum of the air/water interface is shown with the accompanying nonlinear least-squares fit to the data. Each of the contributing vibrations is shown in Figure 6b. Vibrations fit with a negative amplitude are shown in gray, while vibrations with a positive amplitude are shown in black.

Lorentzian distributions generated too much intensity in the 3600 cm^{-1} region of the spectrum, preventing a good fit to the data. A significantly better fit was obtained by considering each transition using the lineshape profile described earlier. The spectra were fit assuming a constant homogeneous or Lorentzian line width Γ of 2 cm^{-1}. The Gaussian or inhomogeneous line width was allowed to vary for each vibration. The spectrum and resulting fit are shown in Figure 6. Each of the vibrations included has a spectroscopic assignment and is expected to arise in the spectrum, but the inclusion of so many overlapping vibrations in the fit makes it difficult to give physical meaning to the specific parameters obtained for each vibration, particularly in the low-frequency region of the spectrum. Information derived from the spectral fit is collected in Table 2. The orientational information is generated assuming that the hydrogens giving rise to the free O−H stretch are pointing away from the bulk water ($\theta < 90°$). The interference patterns observed in the spectrum would be the same if the sign (direction) of every peak in the spectrum were inverted. It should also be noted that it was found to be possible to invert the signs of the vibrational amplitudes of the "liquid-phase" water molecules relative to that of the free O−H stretch while still obtaining a good fit of the spectral data, thereby changing the orientational assignments derived. Such fits were judged to give rise to an unphysical intensity ratio for the asymmetric and symmetric stretch for both the liquid-phase and vapor-phase water molecules. Therefore, it is likely that the average orientation of the tetrahedrally hydrogen-bonded liquid-phase water molecules points away from the surface, back toward the bulk. This alignment of water molecules at the interface creates an interfacial potential, a result in agreement with several molecular dynamics calculations.[30−32]

TABLE 2: Fit Parameters and Orientations Determined for the Air/Water System[a]

	frequency (ω_v)[b]	width (Γ_v)[b]	amplitude (A_v)	orientation
SS−S (icelike)	3170	100	−0.41	$\theta > 90°$
SS−A (liquidlike)	3310	110	−0.41	$\theta > 90°$
AS−"bonded H_2O"	3510	80	0.315	$\theta > 90°$
SS−vapor	3662	23	−0.21	$\theta > 90°$
free OH	3710	27.5	0.42	$\theta < 90°$
AS−vapor	3763	25	0.14	$\theta > 90°$

[a] Results from a nonlinear least-squares fit to the VSF spectrum of the CCl_4/water interface are shown. The spectrum was fit as described in the text. The phase (amplitude) of the free OH vibration is assigned a positive value. As described in the text, it should be noted that some flexibility in adjusting individual parameters can give rise to equally good fits. [b] Frequencies and widths are in units of cm^{-1}.

An examination of the free O−H stretching region of the spectrum (Figure 6) obtained by Allen et al.[9] reveals two previously unassigned transitions, a pair of small vibrations on either side the larger free O−H stretch. These transitions, through analogy with the CCl_4/water interface, are assigned to the symmetric and asymmetric stretch of loosely associated water molecules. The spectral fit reveals that the symmetric stretch has the opposite sign (out-of-phase) and the asymmetric stretch the same sign (in-phase) as the free O−H stretch, indicating that these "vapor-phase" water molecules are aligned with their hydrogens pointing toward the interface. These water molecules are near enough to the interface to show an average orientation aligned with the interfacial potential generated by the asymmetry of the hydrogen-bond network at the surface, but far enough away to show no sign of hydrogen bonding. To our knowledge, this is the first spectroscopic observation of this interesting "phase" of water.

Conclusions

Global fits of the sum frequency spectra of the CCl_4/water and the air/water interfaces are reported. Vibrational modes from liquid-phase, surface, and vapor-phase water molecules are observed in both spectra, allowing the relative intensities and phase differences to be determined. The coherent nature of the sum frequency spectroscopic technique allows the average orientation of molecules contributing to a specific vibrational mode to be determined. The combination of frequency and orientational information obtained from vibrational sum frequency spectra provides a powerful tool in the understanding of the structure of the hydrogen-bond network at water interfaces. To fully understand the sum frequency spectra of water, one must go through such an analysis.

These spectra and the resulting analysis have pulled together for the first time spectra of water at two different interfaces using an analysis that correctly incorporates the phase information carried by the interference of different vibrations. It is hoped that such spectra and analyses will help in the understanding of this complex and interesting liquid.

Acknowledgment. The authors gratefully acknowledge the support of the National Science Foundation for this work.

References and Notes

(1) Du, Q.; Freysz, E.; Shen, Y. R. *Science* **1994**, *264*, 826.
(2) Du, Q.; Superfine, R.; Freysz, E.; Shen, Y. R. *Phys. Rev. Lett.* **1993**, *70*, 2313.

(3) Eisenthal, K. B. *Acc. Chem. Res.* **1993**, *26*, 636.
(4) Eisenthal, K. B. *Chem. Rev.* **1996**, *96*, 1343.
(5) Bain, C. D. *J. Chem. Soc., Faraday Trans.* **1995**, *91*, 1281.
(6) Shen, Y. R. *The Principles of Nonlinear Optics*, 1st ed.; John Wiley & Sons: New York, 1984.
(7) Wolfrum, K.; Laubereau, A. *Chem. Phys. Lett.* **1994**, *228*, 83.
(8) Lobau, J.; Wolfrum, K. *J. Opt. Soc. Am. B* **1997**, *14*, 2505.
(9) Allen, H. C.; Raymond, E. A.; Brown, M. G.; Richmond, G. L., manuscript in preparation.
(10) Scatena, L. F.; Richmond, G. L., manuscript in preparation.
(11) Gragson, D. E.; McCarty, B. M.; Richmond, G. L. *J. Am. Chem. Soc.* **1997**, *119*, 6144.
(12) Messmer, M. C.; Conboy, J. C.; Richmond, G. L. *J. Am. Chem. Soc.* **1995**, *117*, 8039.
(13) Scherer, J. R. *Advances in Infrared and Raman Spectroscopy*; Clark, R. J. H., Hester, R. E., Eds.; Heyden: Philadelphia, PA, 1978; Vol. 5; Chapter 3.
(14) Eisenberg, D.; Kauzmann, W. *The Structure and Properties of Water.*; Oxford University Press: New York, 1969.
(15) Franks, F. *Water: A Comprehensive Treatise*; Plenum Press: New York, 1972; Vol. 1.
(16) Hirose, C.; Akamatsu, N.; Domen, K. *Appl. Spectrosc.* **1992**, *46*, 1051.
(17) Hirose, C.; Akamatsu, N.; Domen, K. *J. Chem. Phys.* **1992**, *96*, 997.
(18) Baldelli, S.; Schnitzer, C.; Shultz, M. J.; Campbell, D. J. *J. Phys. Chem. B* **1997**, *101*, 10435.
(19) Gragson, D.; Richmond, G. *J. Phys. Chem. B* **1998**, *102*, 3847.
(20) Schreier, F. *J. Quant. Spectrosc. Radiat. Transfer* **1992**, *48*, 743.
(21) Goates, S. R.; Schofield, D. A.; Bain, C. D. *Langmuir* **1999**, *15*, 1400.
(22) Feynman, R. P.; Leighton, R. B.; Sands, M. L. *The Feynman Lectures on Physics*; Addison-Wesley: Reading, MA, 1963.
(23) Fredkin, D. R.; Komornicki, A.; White, S. R.; Wilson, K. R. *J. Chem. Phys.* **1983**, *78*, 7077.
(24) Scatena, L. F.; Richmond, G. L., manuscript in preparation.
(25) Gragson, D. E.; McCarty, B. M.; Richmond, G. L. *J. Opt. Soc. Am. B* **1996**, *13*, 2075.
(26) Gragson, D. E.; Alavi, D. S.; Richmond, G. L. *Opt. Lett.* **1995**, *20*, 1991.
(27) Robinson, G. W.; Zhu, S.-B.; Evans, M. W. *Water in Biology, Chemistry and Physics;* World Scientific Publishing Company: London, 1996.
(28) Walrafen, G. E. *The Physics and Physical Chemistry of Water*; Franks, F., Ed.; Plenum Press: New York, 1972.
(29) Chang, T.; Dang, L. X. *J. Chem. Phys.* **1996**, *104*, 6772.
(30) Sokhan, V. P.; Tildesley, D. J. *Mol. Phys.* **1997**, *92*, 625.
(31) Matsumoto, M.; Kataoka, Y. *J. Chem. Phys.* **1988**, *88*, 3233.
(32) Taylor, R. S.; Dang, L. X.; Garrett, B. C. *J. Phys. Chem.* **1996**, *100*, 11720.